

A SEMI-EMPIRICAL MODEL OF STRONG-MOTION PEAKS WITH APPROPRIATE COMPARISONS TO THE 1989 LOMA PRIETA, THE 1985 MICHHOACAN AND THE 1971 SAN FERNANDO EARTHQUAKES

Makoto KAMIYAMA*, Michael J.O'ROURKE**
and Raul FLORES-BERRONES***

This paper deals with strong-motion peaks in terms of seismic source, propagation path and local site conditions. Especially emphasis is placed on the effect of local site conditions. Peak acceleration, peak velocity and peak displacement are analyzed in a similar fashion because they are interrelated. A semi-empirical model is first derived with the aid of seismic source theories and then applied to strong-motion records obtained in Japan. The resulting semi-empirical expressions for the peak acceleration, velocity and displacement are compared with strong-motion data observed during the 1989 Loma Prieta, the 1985 Michoacan and the 1971 San Fernando earthquakes. The semi-empirical expressions explain well the observed strong-motion data in other countries even though they were obtained based solely on Japanese data.

Key Words : strong-motion peak, empirical analysis, seismic source, local site effects

1. INTRODUCTION

Strong earthquake motions are influenced by three main factors : seismic source, propagation path of waves and local site conditions. Therefore peak ground motion parameters, which are usually used for earthquake-resistant design because of their simplicity, should also be estimated in terms of the three factors. In the past, empirical analysis directly or indirectly involving the three factors has been the most common technique for the estimation of peak ground motion parameters. Such analyses have been conducted by many researchers worldwide, presenting different expressions for peak values of motions. An extensive review of empirical prediction of strong ground motions has been recently given by Joyner and Boore¹⁾, being preceded by another comprehensive review of Campbell²⁾ which focused on strong-motion attenuation relations from a statistical standpoint. Although some problems peculiar to empirical prediction of strong motions are pointed out in these reviews along with methods for overcoming such problems, the greatest obstacle for empirical analysis is the limited availability of observed strong motion data. This obstacle is unlikely to easily be resolved because new strong motion records accumulate at a slow pace. Therefore a new technique is necessary to overcome the difficulties of purely empirical prediction methods. In line with

such a necessity, this paper deals with a semi-empirical technique which incorporates information from theoretical seismic source models.

As described in the reviews by Joyner and Boore¹⁾ and by Campbell²⁾, many workers have investigated the influence of local site conditions on peak values of strong motions. Almost all of these investigations use a rough classification scheme such as soft soil, intermediate soil, hard soil and rock without detailed soil profiles specific to individual sites. However a number of actual earthquake damage experiences have taught us that the degree of earthquake damage vary markedly from site to site even within the "soft soil" area. This indicates the importance of individual differences in soil properties at each site. Hence we place emphasis on a technique to obtain site-specific amplification of strong-motion peaks as well as on a semi-empirical model connected with seismic source theories. In this study, peak acceleration, peak velocity and peak displacement in the horizontal direction are analyzed in a similar fashion because they are interrelated.

2. MODEL OF THE SEMI-EMPIRICAL ANALYSIS

For the convenience and simplicity in practical use, we select earthquake magnitude M and hypocentral distance r as the independent variables representing the effects of seismic source and propagation path. In the case of such a selection, it is important to give statistical consideration to the parameters M and r because they are generally correlated in strong-motion data. In particular, since the attenuation coefficient with respect to r is strongly influenced by the correlation between M and r , one needs to pay special attention to the

* Member of JSCE, Dr. Eng., Prof., Dept. of Civil Eng., Tohoku Institute of Technology (35-1 Yagiyama Kasumicho, Sendai 982, Japan)

** Ph.D., Prof., Dept. of Civil and Environment Eng., Rensselaer Polytechnic Institute (RPI) (Troy, New York 12180-3590, USA)

*** Ph.D., Visiting Prof., Dept. of Civil and Environment Eng., RPI

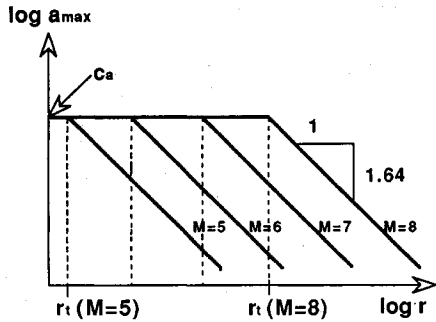


Fig.1(a) Proposed model for peak horizontal ground acceleration as function of hypocentral distance and magnitude

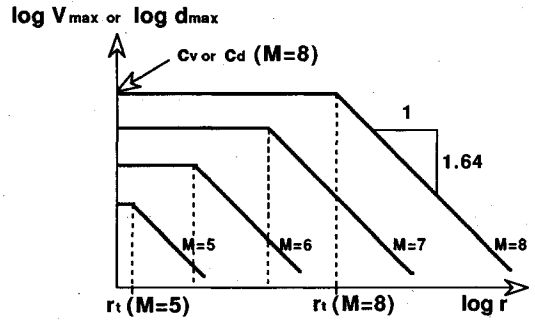


Fig.1(b) Proposed model for peak horizontal ground velocity and displacement as function of hypocentral distance and magnitude

derivation of the attenuation coefficient³⁾. In stead of obtaining by regression analysis, we base our attenuation manner on a coefficient which was carefully derived by the Japan Meteorological Agency (JMA). JMA obtained a value of 1.64 as the distance attenuation for peak velocity⁴⁾. This value was obtained from the Japanese earthquake data satisfying the far field condition which is needed for our semi-empirical model as will be mentioned later. Accordingly we employ the value of 1.64 as the attenuation with respect to hypocentral distance for peak acceleration, peak velocity and peak displacement, assuming that there is little difference in the attenuations for these motions.

The hypocentral distance used in our model is not necessarily the best choice to quantify source-to-site distance but it was selected purely because of its simplicity in practical use. In addition, earthquake source is not a point but consists of a fault with some extended area. Therefore we need to sophisticate our model, which use simple parameters such as earthquake magnitude and hypocentral distance, so as to match seismic source theories.

According to recent studies of earthquake faults, earthquakes generally occur in a form of multiple-shocks which are triggered by rupture of sub-faults associated with the so-called barriers or asperities⁵⁾. In other words, actual earthquakes can be viewed as the result of multiple point-sources, scattered randomly over the entire fault plane. Since such multiple shocks may occur incoherently over the fault plane, one can assume that the peaks of strong motions on or near the fault area are independent of their locations. That is, peak ground motion on and near the fault would be relatively constant. Beyond the immediate fault area, peak motion decreases with distance due to geometric spreading and inelastic phenomena.

Papageorgiou and Aki⁶⁾ discussed theoretically

the peak values of strong motions in a fault area based on the specific barrier model. They suggested that the average cohesive force distributed on the cohesive zone of their specific barrier model and average slip D are determinant parameters for the peaks, and the peak acceleration a_{max} and peak velocity v_{max} in a fault area are approximately given by the following expressions from Ida⁷⁾.

$$a_{max} \approx \frac{\sigma_c}{\mu} V_r \frac{2}{D} \dots\dots\dots (1)$$

$$v_{max} \approx \frac{\sigma_c}{\mu} V_r \dots\dots\dots (2)$$

where, σ_c is an average cohesive stress in the cohesive zone, D is the average slip in the cohesive zone, V_r is the rupture velocity of fault and μ is the rigidity modulus.

Applying the specific barrier model to earthquakes in California, Chin and Aki⁸⁾ estimated empirically the values of σ_c and D which are associated with earthquake magnitude. The results show that the logarithmic values of both σ_c and D are linearly proportional to earthquake magnitude in a similar manner. This means from Eqs. (1) and (2) that peak acceleration in a fault area is independent of earthquake magnitude while the peak of velocity is proportional to earthquake magnitude since V_r and μ are known to be independent of earthquake magnitude. We employ this assumed characteristics of peak acceleration and peak velocity in a fault zone as an important tool for our semi-empirical model. The fault extent here is identical for both acceleration and velocity and assumed to be an increasing function of the earthquake magnitude. This is based on numerous empirical studies which show that earthquake fault length is an increasing function of earthquake magnitude. Figures of our semi-empirical model due to the above consideration are sketched in Fig.1(a) and (b) for peak acceleration and peak velocity respectively. Note that peak displacement

is assumed to behave in a manner similar to peak velocity.

The parameters c_a , c_v and r_i in Fig.1(a) and Fig.1(b) are determined empirically in accordance with observed earthquake data. We require that the values of r_i be common for the acceleration, velocity and displacement models, since they represent earthquake fault size. Fig.1(a) and Fig.1(b) show clearly that it is easier to first determine r_i from the acceleration data and then apply the values to the more complicated velocity and displacement models whose peaks in the fault region depend on earthquake magnitude. A dummy variable concept, described by Kamiyama and Matsukawa⁹⁾, is herein used to evaluate r_i and c_a . A schematic figure is shown in Fig.2 to illustrate such a dummy variable concept for empirically evaluating r_i and c_a . By setting an arbitrary value r_c , we use a trial and error procedure to obtain final values of r_i and c_a . This dummy variable concept yields a regression model :

$$\log_{10} a_{\max} = -1.64R_0 + b_1R_1 + b_2R_2 + c_a \dots (3)$$

where

$$R_0 = \begin{cases} 0 & (r \leq r_c) \\ \log_{10} r - \log_{10} r_c & (r > r_c) \end{cases} \dots (4)$$

$$R_1 = \begin{cases} 0 & (r \leq r_c) \\ 1 & (r > r_c) \end{cases} \dots (5)$$

$$R_2 = \begin{cases} 0 & (r \leq r_c) \\ M & (r > r_c) \end{cases} \dots (6)$$

and b_1 , b_2 and c_a are regression coefficients. The parameter r_i becomes a function of earthquake magnitude M as

$$r_i = r_c \times 10^{\frac{b_1 + b_2 M}{1.64}} \dots (7)$$

As shown in Eq.(7), the target values r_i and c_a determined by the model of Eq.(3) are dependent on the selected value for the arbitrary variable r_c . The final determination of r_i and c_a is based upon the goodness of fit between predicted and observed of a_{\max} for various values of the arbitrary variable r_c , as well as upon empirical information on earthquake fault size.

The models for peak velocity and displacement in Fig.1(b) are constructed by adding another term controlling the magnitude-dependence of the peak in the fault area and using the regression coefficients b_1 and b_2 in Eq.(3) of the acceleration model. Namely, they are given by

$$\log_{10} v_{\max} = \alpha M - 1.64R_0 + b_1R_1 + b_2R_2 + c_v \dots (8)$$

$$\log_{10} d_{\max} = \delta M - 1.64R_0 + b_1R_1 + b_2R_2 + c_d \dots (9)$$

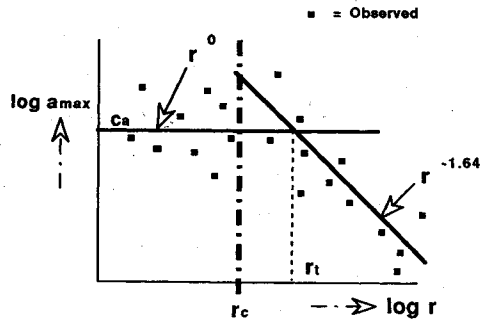


Fig.2 A schematic figure for empirically determining r_i and c_a for the peak acceleration model

where v_{\max} is the peak horizontal velocity, d_{\max} is the peak horizontal displacement, M is the JMA earthquake magnitude, and α , δ , c_v and c_d are regression coefficients, and R_0 , R_1 and R_2 are the same as those in Eqs.(4) to (6).

In Eqs.(8) and (9), only the coefficients, α , δ , c_v and c_d are determined empirically by regression analysis, since the values b_1 and b_2 are determined from the acceleration model.

Eqs.(3), (8) and (9) are semi-empirical models which consists of seismic source characteristics and propagation path. As described above, an additional term is needed to reflect the individual local site effects. We define independent variables to represent local effects at each site as opposed to the rough classification schemes in the past empirical analyses. Kamiyama and Yanagisawa¹⁰⁾ has shown that the concept of dummy variables was effective for individualizing local site effects in their statistical analysis of response spectra. Herein we employ the following model, similar to that for response spectra, in order to empirically obtain the effect of individual local sites :

$$\log_{10} a_{\max} = -1.64R_0 + b_1R_1 + b_2R_2 + c_a + A_1S_1 + A_2S_2 + \dots + A_{N-1}S_{N-1} \dots (10)$$

$$\log_{10} v_{\max} = \alpha M - 1.64R_0 + b_1R_1 + b_2R_2 + c_v + B_1S_1 + B_2S_2 + \dots + B_{N-1}S_{N-1} \dots (11)$$

$$\log_{10} d_{\max} = \delta M - 1.64R_0 + b_1R_1 + b_2R_2 + c_d + D_1S_1 + D_2S_2 + \dots + D_{N-1}S_{N-1} \dots (12)$$

where S_j ($j=1 \sim N-1$) are the dummy variables and A_i , B_i and D_i ($i=1 \sim N-1$) are regression coefficients.

As seen in Eqs.(10) to (12), the $N-1$ independent dummy variables S_j are assigned to all observation sites except a reference site. This technique avoids statistical difficulties and obtains local site amplification factors of the peak values with respect to a reference site. When a reference

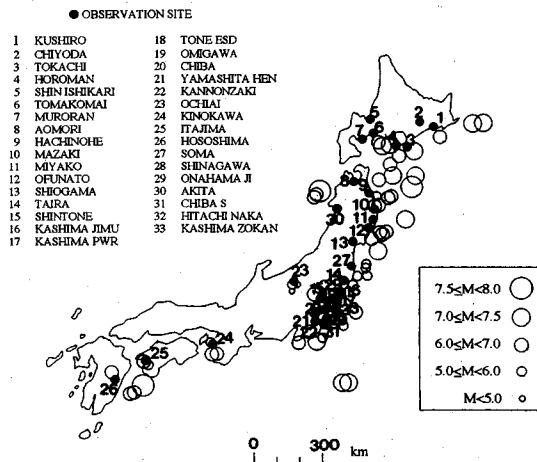


Fig.3 Observation sites and epicenters

site is selected to satisfy the conditions of "seismic bed rock" which is bed rock for seismic response analysis of surface soils, the amplification factors thus obtained have physical meaning. An explanation of such amplification factors is described fully in Kamiyama and Yamagisawa¹⁰. The amplification factors AMP_i for the peak acceleration, velocity and displacement at the i -th site against a reference site are given by

$$AMP_i = 10^{A_i}, 10^{B_i} \text{ or } 10^{D_i} \dots \dots \dots (13)$$

3. EARTHQUAKE DATA USED FOR THE SEMI-EMPIRICAL ANALYSIS

The main purpose of this study is to analyze the effects of individual sites on the strong-motion peaks. Hence we use strong-motion records obtained in Japan, which are relatively rich in records at a specific site during various earthquakes. We collected a total of 357 horizontal strong-motion accelerograms observed by the both Ministries of Transport and Construction of Japan distributing wide observation networks throughout the country^{11,12}. These accelerograms are listed in Kamiyama, O'Rourke and Flores-Berrones³. Fig.3 illustrates the observation sites along with the epicenters of the earthquakes provided these accelerograms. As shown in Fig.3, the total numbers of observation sites and earthquakes are 33 and 82 respectively.

These accelerograms were obtained mostly by the SMAC types of accelerographs. Because the original accelerograms include several errors resulting from the frequency characteristics of instrument, digitization processing, etc., we first removed the errors by performing the frequency

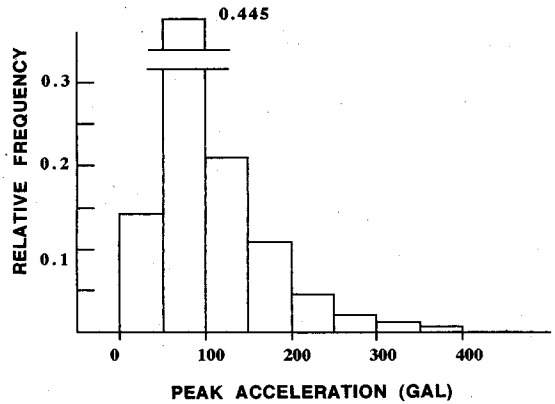


Fig.4 Histogram of peak horizontal ground acceleration used in the analysis

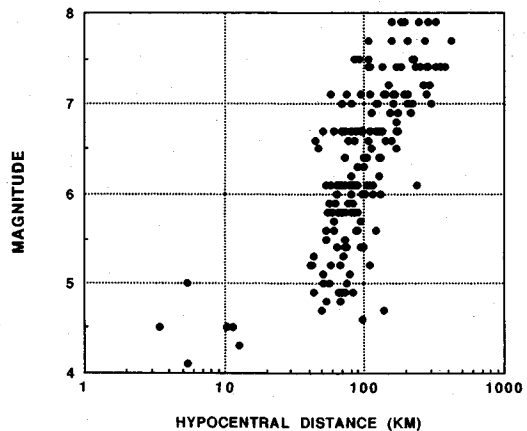


Fig.5 Scattergram of magnitude and hypocentral distance in data

characteristics correction according to each instrument as well as by treating through a band-pass filter. Based on such correction and filtering, corrected acceleration, velocity and displacement records were numerically obtained together with their peak values. The frequency characteristics of the band-pass filter used herein was proposed by Iai et al.¹³ as a standard filter applied to the accelerograms observed by the Transport Ministry. It has a flat part ranging from about 0.09 sec. to about 4.2 sec. This period band should be emphasized when the peak velocity and displacement are examined.

Fig.4 is a histogram for one of the dependent variables; peak horizontal acceleration. The inter-relationship between the independent variables; earthquake magnitude and hypocentral distance is shown in the scattergram in Fig.5. This figure shows strongly positive correlation between the two variables. Hence the data set used herein has some limits from a statistical point of view. These

Table 1 Regression coefficients, multiple correlation coefficient, standard error and r_i for acceleration model

| | r_c (km) | | | | | | | | | | | | | | | |
|------------|------------|--------|--------|--------|--------|--------|--------|--------|--------|--------|--------|--------|--------|--------|--------|--------|
| | 50 | 40 | 30 | 20 | 10 | 8.0 | 6.0 | 5.8 | 5.6 | 5.4 | 5.3 | 5.2 | 5.1 | 4.8 | 4.6 | 4.4 |
| b_1 | -1.766 | -1.760 | -1.555 | -1.266 | -0.767 | -0.608 | -0.403 | -0.379 | -0.354 | -0.819 | -1.164 | -1.150 | -1.137 | -1.093 | -1.063 | -1.031 |
| b_2 | 0.324 | 0.333 | 0.333 | 0.333 | 0.332 | 0.332 | 0.332 | 0.332 | 0.332 | 0.345 | 0.358 | 0.358 | 0.358 | 0.358 | 0.358 | 0.358 |
| c_a | 2.126 | 2.228 | 2.228 | 2.228 | 2.228 | 2.228 | 2.283 | 2.228 | 2.228 | 2.637 | 2.910 | 2.910 | 2.910 | 2.910 | 2.910 | 2.910 |
| R | 0.845 | 0.854 | 0.862 | 0.876 | 0.896 | 0.900 | 0.905 | 0.906 | 0.906 | 0.894 | 0.890 | 0.890 | 0.890 | 0.891 | 0.891 | 0.891 |
| S | 0.228 | 0.227 | 0.227 | 0.227 | 0.228 | 0.228 | 0.228 | 0.228 | 0.228 | 0.243 | 0.247 | 0.247 | 0.247 | 0.247 | 0.247 | 0.247 |
| r_i (km) | M=5 | 41.3 | 35.1 | 35.1 | 35.1 | 35.1 | 35.1 | 35.1 | 35.1 | 19.3 | 12.8 | 12.8 | 12.8 | 12.8 | 12.8 | 12.8 |
| | M=6 | 65.1 | 56.0 | 56.0 | 56.0 | 56.0 | 56.0 | 56.0 | 56.0 | 31.3 | 21.2 | 21.2 | 21.2 | 21.2 | 21.2 | 21.2 |
| | M=7 | 102.6 | 89.4 | 89.4 | 89.4 | 89.3 | 89.3 | 89.3 | 89.3 | 50.8 | 35.0 | 34.9 | 34.9 | 35.0 | 35.0 | 35.0 |
| | M=8 | 161.7 | 142.8 | 142.8 | 142.8 | 142.5 | 142.5 | 142.5 | 142.5 | 82.5 | 57.9 | 57.8 | 57.8 | 57.9 | 57.9 | 57.9 |

b_1, b_2 and c_a =regression coefficients, M= earthquake magnitude
 R =multiple correlation coefficient
 S = standard error
 $r_i = r_c \times 10^{\frac{b_1 + b_2 M}{1.64}}$

limits provided motivation for the semi-empirical model as stated in the foregoing section.

4. REGRESSION ANALYSIS OF THE SEMI-EMPIRICAL MODELS

Our regression analyses consist of two phases. In the first phase the appropriate values of r_i are determined using the acceleration model of Eq.(10). In the second phase the velocity and displacement models are established using the results for r_i from the acceleration model. In addition, we need to assign a reference site. Such a reference site, of course, can be picked arbitrarily from any of the observation sites. However our previous study¹⁰⁾ reveals that it is most desirable to assign a site where there exists outcrop hard enough to satisfy the condition of the seismic bed rock for the other sites. Although the selection of the seismic bed rock might vary according to the dominant frequency content, we initially selected the same reference site for the acceleration, velocity and displacement models on the condition that the definition of the seismic bed rock should be examined based on the resulting amplification factors at each observation site. Herein we choose OFUNATO labeled 12 in Fig.3 as the reference site in accordance with the discussion in Kamiyama and Yanagisawa¹⁰⁾. The OFUNATO site is situated at a rock outcrop having shear wave velocity in the 1 to 2 km/sec range.

Table 1 shows the summary of the regression coefficients analyzed for trial values of r_c in the acceleration model. Note that the multiple correlation coefficient R , which means the goodness of fit, is largest for $r_c < 10$ km. Table 1 also shows that the variation of r_i depends on r_c but it becomes relatively stable for $r_c \leq 5.3$ km. As stated in the

Table 2 Fault radius based on the Sato[14] relation for fault area

| MAGNITUDE M | RADIUS (KM) |
|----------------|----------------|
| 5 | 1.65 |
| 6 | 5.21 |
| 7 | 16.46 |
| 8 | 52.05 |

preceding section, r_i is closely related to a characteristic length of the earthquake fault. Hence in addition to the goodness of fit and stability of the r_i parameter, the choice of b_1 and b_2 is also based on the consistency of r_i with empirical estimates of fault length. Although the value of r_i is somewhat arbitrarily related to fault length, it is reasonable to interpret r_i as nearly equivalent to the radius of the fault which is assumed herein to be circular. The fault area of earthquake has been investigated by many workers. Typically it is related to earthquake magnitude. For instance, Sato¹⁴⁾ derived the following expression.

$$S = 10^{M-4.07} \dots \dots \dots (14)$$

where S is the area of the fault in square kilometers.

Table 2 shows the variation of fault radius obtained from Eq.(14) assuming a circular fault. A comparison between Table 1 and Table 2 indicates that values of r_c less than or equal to 5.3 km yield the best match between r_i and empirical estimates of the fault radius by others, even though there is a relatively big difference between them in smaller earthquake magnitude. The difference may be due to the possibility that r_i is related to a characteristic length of a rectangular fault rather than the radius of circular fault. Accordingly, we choose $b_1 = -1.164$, $b_2 = 0.358$ and $c_a = 2.91$, which were obtained by setting $r_c = 5.3$ km, for the acceleration

Table 3 Site amplification coefficients for acceleration model

| NO | SITE NAME | A _i |
|----|---------------|----------------|
| 1 | KUSHIRO | 0.196 |
| 2 | CHIYODA | 0.127 |
| 3 | TOKACHI | 0.110 |
| 4 | HOROMAN | -0.202 |
| 5 | SHIN ISHIKARI | 0.396 |
| 6 | TOMAKOMAI | 0.129 |
| 7 | MURORAN | 0.271 |
| 8 | AOMORI | 0.090 |
| 9 | HACHINOHE | -0.098 |
| 10 | MAZAKI | -0.092 |
| 11 | MIYAKO | 0.194 |
| 12 | OFUNATO | ----- |
| 13 | SHIOGAMA | 0.193 |
| 14 | TAIRA | 0.046 |
| 15 | SHINTONE | -0.092 |
| 16 | KASHIMA JIMU | -0.002 |
| 17 | KASHIMA PWR | -0.047 |
| 18 | TONE ESD | -0.139 |
| 19 | OMIGAWA | -0.104 |
| 20 | CHIBA | 0.021 |
| 21 | YAMASHITA HEN | -0.123 |
| 22 | KANNONZAKI | 0.129 |
| 23 | OCHIAI C | -0.768 |
| 24 | KINOKAWA | -0.771 |
| 25 | ITAJIMA | 0.349 |
| 26 | HOSOSHIMA | -0.113 |
| 27 | SOMA | 0.239 |
| 28 | SHINAGAWA | 0.032 |
| 29 | ONAHAMA JI | 0.076 |
| 30 | AKITA | -0.037 |
| 31 | CHIBA S | -0.032 |
| 32 | HITACHI NAKA | 0.135 |
| 33 | KASHIMA ZOKAN | 0.016 |

Table 4 Regression coefficients, site amplification coefficients, multiple coefficient and standard error for velocity and displacement models

| REGRESSION COEFFICIENTS | | MAX VEL | MAX DIS |
|---------------------------------|---------------|---------|---------|
| α, δ | | 0.153 | 0.236 |
| b ₁ | | -1.164 | -1.164 |
| b ₂ | | 0.358 | 0.358 |
| c _v , c _d | | 0.333 | -0.322 |
| B _i , D _i | | | |
| 1 | KUSHIRO | 0.431 | 0.343 |
| 2 | CHIYODA | 0.296 | 0.294 |
| 3 | TOKACHI | 0.127 | 0.151 |
| 4 | HOROMAN | -0.295 | -0.302 |
| 5 | SHIN ISHIKARI | 0.748 | 0.662 |
| 6 | TOMAKOMAI | 0.255 | 0.241 |
| 7 | MURORAN | 0.313 | 0.213 |
| 8 | AOMORI | 0.488 | 0.494 |
| 9 | HACHINOHE | 0.131 | 0.176 |
| 10 | MAZAKI | 0.039 | 0.409 |
| 11 | MIYAKO | 0.033 | -0.034 |
| 12 | OFUNATO | ----- | ----- |
| 13 | SHIOGAMA | 0.465 | 0.161 |
| 14 | TAIRA | 0.310 | 0.282 |
| 15 | SHINTONE | 0.298 | 0.204 |
| 16 | KASHIMA JIMU | 0.364 | 0.239 |
| 17 | KASHIMA PWR | 0.294 | 0.089 |
| 18 | TONE ESD | 0.346 | 0.568 |
| 19 | OMIGAWA | 0.337 | 0.587 |
| 20 | CHIBA | 0.314 | 0.432 |
| 21 | YAMASHITA HEN | 0.116 | 0.051 |
| 22 | KANNONZAKI | 0.179 | 0.067 |
| 23 | OCHIAI C | -0.534 | -0.641 |
| 24 | KINOKAWA | -0.568 | -0.630 |
| 25 | ITAJIMA | 0.356 | 0.207 |
| 26 | HOSOSHIMA | 0.051 | -0.118 |
| 27 | SOMA | 0.110 | -0.088 |
| 28 | SHINAGAWA | 0.358 | 0.136 |
| 29 | ONAHAMA JI | 0.112 | 0.099 |
| 30 | AKITA | 0.227 | 0.248 |
| 31 | CHIBA S | 0.342 | 0.176 |
| 32 | HITACHI NAKA | 0.053 | -0.496 |
| 33 | KASHIMA ZOKAN | 0.133 | 0.050 |
| MULTIPLE CORRELATION COEFFICI. | | 0.770 | 0.848 |
| STANDARD ERROR | | 0.264 | 0.272 |

model of Eq.(10). The regression coefficients A₁, A₂, ..., A_{N-1} in Eq.(10), which were obtained based on r_c=5.3, are shown in Table 3. In Table 3, A_i (i = 1 ~ N-1) are given for each observation site except the reference site. Hence the eventual semi-empirical expression for the peak horizontal ground acceleration is

$$a_{\max}(i, M, r) = 10^{2.910 + A_i} \dots (15)$$

$$\text{for } (r \leq 10^{0.014 + 0.218M})$$

$$a_{\max}(i, M, r) = 10^{2.933 + 0.358M - 1.64 \log_{10} r} \times 10^{A_i}$$

$$\text{for } (r > 10^{0.014 + 0.218M}) \dots (16)$$

where A_i are given in Table 3 on the condition that A_i=0 for the reference site.

The regression coefficients of the velocity and displacement models of Eqs.(11) and (12) are presented in Table 4 based on b₁=-1.164 and b₂=0.358 from the acceleration model. Hence the semi-empirical expressions for the peak horizontal ground velocity and displacement are

$$v_{\max}(i, M, r) = 10^{0.535 + 0.153M} \times 10^{B_i}$$

$$\text{for } (r \leq 10^{0.014 + 0.218M}) \dots (17)$$

$$v_{\max}(i, M, r) = 10^{0.558 + 0.511M - 1.64 \log_{10} r} \times 10^{B_i}$$

$$\text{for } (r > 10^{0.014 + 0.218M}) \dots (18)$$

$$d_{\max}(i, M, r) = 10^{-0.522 + 0.236M} \times 10^{D_i}$$

$$\text{for } (r \leq 10^{0.014 + 0.218M}) \dots (19)$$

$$d_{\max}(i, M, r) = 10^{-0.499 + 0.594M - 1.64 \log_{10} r} \times 10^{D_i}$$

$$\text{for } (r > 10^{0.014 + 0.218M}) \dots (20)$$

where B_i and D_i are given in Table 4 on the condition that B_i=0 or D_i=0 for the reference site.

Finally, adequacy of the semi-empirical model was checked statistically by inspection of the residuals plots. The residuals, which are simply the ratio of the observed to predicted velocities from Eqs.(17) and (18), were plotted as functions of peak velocity, as an example, is illustrated in terms of earthquake magnitude in Fig.6. The fact that no particular trend was observed in the residual plots implies that the proposed semi-empirical model is adequate from a statistical point of view.

5. AMPLIFICATION DUE TO LOCAL SITE CONDITIONS

Table 5 lists the amplification factors obtained for the peak acceleration, velocity and displacement at each site along with their mean values and standard deviations. In Table 5, the amplification factor at the reference site (OFUNATO) is set to be one by definition. We can see from Table 5 that

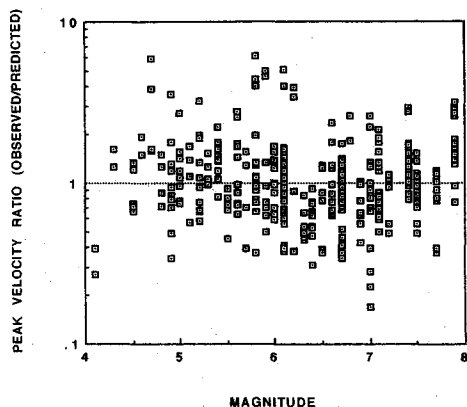


Fig.6 Residual plots of peak velocity versus magnitude

Table 5 Amplification factors for peak acceleration, peak velocity and peak displacement

| NO | SITE NAME | AMPLIFICATION FACTORS | | |
|-------|--------------------|-----------------------|-------|-------|
| | | ACC | VEL | DIS |
| 1 | KUSHIRO | 1.57 | 2.70 | 2.21 |
| 2 | CHIYODA | 1.30 | 1.98 | 1.97 |
| 3 | TOKACHI | 1.29 | 1.34 | 1.42 |
| 4 | HOROMAN | 0.63 | 0.51 | 0.50 |
| 5 | SHIN ISHIKARI | 2.49 | 5.59 | 4.67 |
| 6 | TOMAKOMAI | 1.35 | 1.80 | 1.74 |
| 7 | MURORAN | 1.86 | 2.05 | 1.63 |
| 8 | AOMORI | 1.23 | 3.08 | 3.12 |
| 9 | HACHINOHE | 0.80 | 1.35 | 1.50 |
| 10 | MAZAKI | 0.81 | 1.09 | 2.56 |
| 11 | MIYAKO | 1.56 | 1.08 | 0.92 |
| 12 | OFUNATO | 1.00 | 1.00 | 1.00 |
| 13 | SHIOGAMA | 1.56 | 2.91 | 1.45 |
| 14 | TAIRA | 1.11 | 2.04 | 1.91 |
| 15 | SHINTONE | 0.81 | 1.99 | 1.60 |
| 16 | KASHIMA JIMU | 1.00 | 2.31 | 1.73 |
| 17 | KASHIMA PWR | 0.89 | 1.97 | 1.23 |
| 18 | TONE ESD | 0.73 | 2.27 | 3.70 |
| 19 | OMIGAWA | 0.79 | 2.27 | 3.86 |
| 20 | CHIBA | 1.05 | 2.06 | 2.70 |
| 21 | YAMASHITA HEN | 0.76 | 1.45 | 1.12 |
| 22 | KANNONZAKI | 1.35 | 1.51 | 1.17 |
| 23 | OCHIAI C | 0.17 | 0.29 | 0.23 |
| 24 | KINOKAWA | 0.17 | 0.28 | 0.22 |
| 25 | ITAJIMA | 2.23 | 2.27 | 1.61 |
| 26 | HOSOSHIMA | 0.74 | 1.12 | 0.76 |
| 27 | SOMA | 1.73 | 1.29 | 0.82 |
| 28 | SHINAGAWA | 1.08 | 2.28 | 1.37 |
| 29 | ONAHAMA JI | 1.19 | 1.31 | 1.26 |
| 30 | AKITA | 0.92 | 1.68 | 1.77 |
| 31 | CHIBA S | 0.93 | 2.20 | 1.50 |
| 32 | HITACHI NAKA | 1.36 | 1.13 | 0.32 |
| 33 | KASHIMA ZOKAN | 1.03 | 1.36 | 1.12 |
| ----- | Average | 1.136 | 1.805 | 1.657 |
| ----- | Standard deviation | 0.497 | 0.965 | 1.027 |

the amplification factors vary markedly from site to site probably reflecting the difference in the soil conditions. In addition, the variations of the amplification factors differ depending on the type of motion characteristics : acceleration, velocity and displacement. This significant variation in amplification factors indicates the importance of taking individual site conditions into consideration, as contrasted with the rough classification schemes of soil conditions employed in the past studies.

The same reference site was selected for all three motions; acceleration, velocity and displacement. However, the difference in the variations of amplification factors for the three motions indicates that the reference site should be selected

Table 6 Renovated amplification factors for peak acceleration, peak velocity and peak displacement

| NO | SITE NAME | RENOVATED AMPLIFICATION FACTORS | | |
|-------|--------------------|---------------------------------|-------|-------|
| | | ACC | VEL | DIS |
| 1 | KUSHIRO | 2.46 | 3.21 | 3.51 |
| 2 | CHIYODA | 2.03 | 2.36 | 3.13 |
| 3 | TOKACHI | 2.02 | 1.60 | 2.25 |
| 4 | HOROMAN | 0.99 | 0.61 | 0.79 |
| 5 | SHIN ISHIKARI | 3.90 | 6.66 | 7.41 |
| 6 | TOMAKOMAI | 2.11 | 2.14 | 2.76 |
| 7 | MURORAN | 2.91 | 2.44 | 2.59 |
| 8 | AOMORI | 1.92 | 3.67 | 4.95 |
| 9 | HACHINOHE | 1.25 | 1.61 | 2.38 |
| 10 | MAZAKI | 1.27 | 1.30 | 4.06 |
| 11 | MIYAKO | 2.44 | 1.23 | 1.46 |
| 12 | OFUNATO | 1.56 | 1.19 | 1.59 |
| 13 | SHIOGAMA | 2.44 | 3.46 | 2.30 |
| 14 | TAIRA | 1.74 | 2.43 | 3.03 |
| 15 | SHINTONE | 1.27 | 2.37 | 2.54 |
| 16 | KASHIMA JIMU | 1.56 | 2.75 | 2.75 |
| 17 | KASHIMA PWR | 1.39 | 2.35 | 1.95 |
| 18 | TONE ESD | 1.14 | 2.70 | 5.87 |
| 19 | OMIGAWA | 1.24 | 2.70 | 6.13 |
| 20 | CHIBA | 1.64 | 2.45 | 4.29 |
| 21 | YAMASHITA HEN | 1.19 | 1.73 | 1.78 |
| 22 | KANNONZAKI | 2.11 | 1.80 | 1.86 |
| 23 | OCHIAI C | 0.27 | 0.35 | 0.37 |
| 24 | KINOKAWA | 0.27 | 0.33 | 0.35 |
| 25 | ITAJIMA | 3.49 | 2.70 | 2.56 |
| 26 | HOSOSHIMA | 1.16 | 1.33 | 1.21 |
| 27 | SOMA | 2.71 | 1.54 | 1.30 |
| 28 | SHINAGAWA | 1.69 | 2.71 | 2.17 |
| 29 | ONAHAMA JI | 1.86 | 1.56 | 2.00 |
| 30 | AKITA | 1.44 | 2.00 | 2.81 |
| 31 | CHIBA S | 1.46 | 2.62 | 2.38 |
| 32 | HITACHI NAKA | 2.13 | 1.35 | 0.51 |
| 33 | KASHIMA ZOKAN | 1.61 | 1.62 | 1.78 |
| ----- | Average | 1.778 | 2.149 | 2.630 |
| ----- | Standard deviation | 0.778 | 1.149 | 1.630 |

differently depending on the motion characteristics. Note that, for example, the average amplification factor for the peak acceleration is only slightly larger than 1.0 which is the amplification factor for the reference site, whereas the average amplification factors for the peak velocity and displacement are roughly 1.8 and 1.7 respectively. Since local soil conditions generally amplify the motions incident to the seismic bed rock, the amplification factor is expected to be greater than 1.0 when the reference site is properly selected to satisfy the condition of the seismic bed rock. Considering that we have obtained meaningful amplification factors as relative values even though they are controversial in the absolute values, we renovate the amplification factors in Table 5 so as to meet a proper condition of amplification. Herein we make an attempt by renovating the amplification factors in Table 5 so that the average value minus the one standard deviation is 1.0. For example, $1/(1.136-0.497)$ is multiplied to the amplification factors in the case of the peak acceleration. This is an attempt to make the amplification factors approach proper values with respect to the seismic bed rock. The amplification factors for the peak velocity and peak displacement were also renovated in a similar manner. The final amplification factors for each motion peak are listed in Table 6. Note in Table 6 that the definition of the seismic bed rock differs for peak acceleration, velocity and displacement as

a result of the renovations. For example, HOROMAN, OFUNATO and HOROMAN correspond to the seismic bed rock site for the peak acceleration, velocity and displacement respectively because their renovated amplification factors are nearly equal to 1.0. A geological survey shows a rock outcrop at the HOROMAN site as well as OFUNATO. It is noted in **Table 6** that several observation sites such as OCHIAI and KINOKAWA give small amplification factors. One possible reason leading to such small amplifications is that some of the strong-motion records at these sites are lacking in a part of main-motions. However the amplification factors are also associated with the soil conditions, so this problem should be further studied considering the relation between the amplification factors and soil conditions.

As a result of the renovations for the amplification factors, the overall semi-empirical expressions of Eqs.(15) to (20) are modified so that the motion peaks on the seismic bed rock are diminished to offset the increased amplification factors resulting from the renovations. Denoting the renovated amplification factors at the i -th site in **Table 6** as $AMP_i(a)$, $AMP_i(v)$ and $AMP_i(d)$ for the peak acceleration, peak velocity and peak displacement respectively, we rewrite the final semi-empirical expressions as follows :

$$a_{\max}(i, M, r) = 518.9 \times AMP_i(a) \quad \text{for } (r \leq 10^{0.014+0.218M}) \dots\dots\dots (21)$$

$$a_{\max}(i, M, r) = 547.6 \times 10^{0.358M - 1.64 \log_{10} r} \times AMP_i(a) \quad \text{for } (r > 10^{0.014+0.218M}) \dots\dots\dots (22)$$

$$v_{\max}(i, M, r) = 2.879 \times 10^{0.153M} \times AMP_i(v) \quad \text{for } (r \leq 10^{0.014+0.218M}) \dots\dots\dots (23)$$

$$v_{\max}(i, M, r) = 3.036 \times 10^{0.511M - 1.64 \log_{10} r} \times AMP_i(v) \quad \text{for } (r > 10^{0.014+0.218M}) \dots\dots\dots (24)$$

$$d_{\max}(i, M, r) = 0.189 \times 10^{0.236M} \times AMP_i(d) \quad \text{for } (r \leq 10^{0.014+0.218M}) \dots\dots\dots (25)$$

$$d_{\max}(i, M, r) = 0.200 \times 10^{0.594M - 1.64 \log_{10} r} \times AMP_i(d) \quad \text{for } (r > 10^{0.014+0.218M}) \dots\dots\dots (26)$$

where a_{\max} is peak horizontal acceleration (cm/sec²), v_{\max} is peak horizontal velocity (cm/sec), d_{\max} is peak horizontal displacement (cm), i is the number for identifying the observation site, M is the JMA earthquake magnitude, and r is the hypocentral distance (km).

6. COMPARISON BETWEEN THE PROPOSED MODEL AND OBSERVATIONS DURING EARTHQUAKES IN OTHER COUNTRIES

We can see from Eqs.(21) to (26) how the strong motions depend on local site effects as well as earthquake magnitude and source-to-site distance. The site amplifications vary from site to site reflecting the soil profiles at each site. A close relation between the site amplification and soil profile has been discussed in detail by Kamiyama, O'Rourke and Flores-Berrones³⁾, leading to a technique of estimating amplification factor at a new site not involved in the analyses of this study. On the other hand, Eqs.(21) to (26) provides us with an estimate of peak values of strong motions on the "seismic bed rock", which is bed rock for seismic response analysis of surface soils, with the exception of amplification factors $AMP_i(a)$, $AMP_i(v)$ and $AMP_i(d)$. Such a rock site estimate is significant because we usually need strong motions at rock sites in the design of important structures such as nuclear power plants. At the same time we derived our semi-empirical expressions of strong-motion peaks merely based on the Japanese data. Hence it is of interest to compare the results with observed strong-motion data obtained in other countries for the purpose of confirming the validity of the proposed semi-empirical model. In this paper, we investigate the validity of the proposed model by comparing its predicted results with the strong-motion data observed during the 1989 Loma Prieta earthquake, the 1985 Michoacan earthquake and the 1971 San Fernando earthquake. These earthquakes were chosen because they offer strong-motion records from both the near field and far field. We picked strong-motion data observed at rock sites during these earthquakes and compared them with the predicted values from the proposed semi-empirical model. Since we consider only rock sites in the comparisons, $AMP_i(a)$, $AMP_i(v)$ and $AMP_i(d)$ were set equal to one in Eqs.(21) through (26). In the comparisons, the earthquake magnitude scale in other countries was regarded as identical to the JMA magnitude scale employed in the proposed model in consideration of some statistical errors involved in any definition of earthquake magnitude.

Fig.7 to 15 show respectively the comparisons between the observed and predicted peak accelerations, peak velocities and peak displacements. In each figure, the error bands of prediction based on the one standard error of the regression analyses

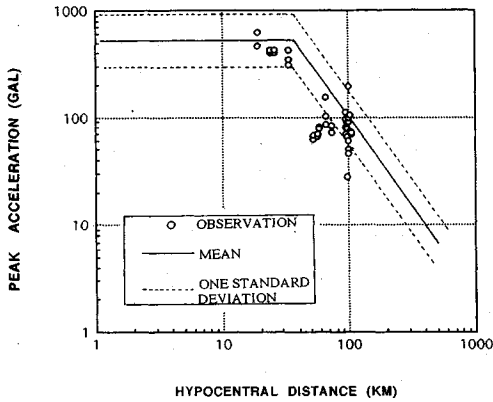


Fig. 7 Comparison of peak acceleration at rock sites for the 1989 Loma Prieta earthquake with value predicted by the proposed semi-empirical model for $M=7.0$

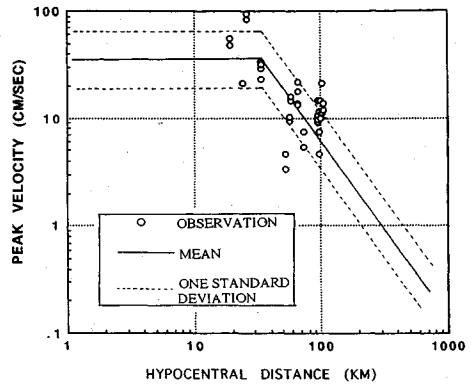


Fig. 8 Comparison of peak velocity at rock sites for the 1989 Loma Prieta earthquake with value predicted by the proposed semi-empirical model for $M=7.0$

are plotted in addition to predicted mean values. The standard error for the the peak acceleration analysis is shown in **Table 1** ($r_c=5.3$ km) and those for the peak velocity and displacement are shown in **Table 4**. Note that there is a relatively good agreement between the observed and predicted values in **Figs. 7 to 15**, especially for peak velocity of **Figs. 8, 11 and 14**. Since the proposed model does not use earthquake fault parameters like rupture directivity but uses only simple parameters such as earthquake magnitude and hypocentral distance, some discrepancy between the observed and predicted values is inevitable. However most of the observed peak values are distributed within the error band of the prediction except a comparison of peak acceleration for the San Fernando event.

Despite a relatively good agreement in the overall comparisons, there is disparity between the observed and predicted values for the near field of the 1985 Michocan earthquake and the peak acceleration of the 1971 San Fernando earthquake. The disparity is attributable to several reasons including incompleteness of the model and the peculiarities of each earthquake. Some of the incompleteness result from the simplification of the proposed model being developed for engineering purpose. In particular, the proposed model does not consider the faulting process at the seismic source which affects peak values of strong-motions. The introduction of faulting parameters to empirical model of strong-motion peaks is an open question for possible further study.

7. SUMMARY AND CONCLUSIONS

This study dealt with a semi-empirical model for estimating the peak values of strong motions with

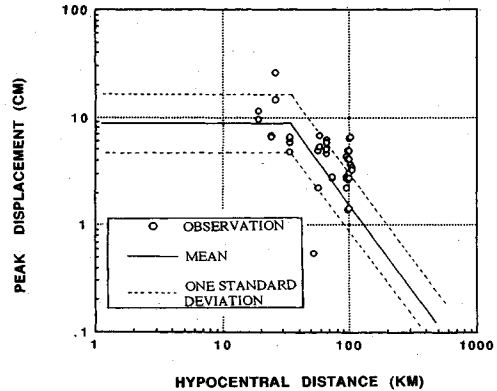


Fig. 9 Comparison of peak displacement at rock sites for the 1989 Loma Prieta earthquake with value predicted by the proposed semi-empirical model for $M=7.0$

emphasis on local site effects. In the derivation of the model, theoretical information about seismic sources was combined with a statistical analysis of strong-motion data from Japan. The concept of dummy variables was used to obtain amplification factors due to individual local site conditions in the statistical analysis.

The amplification factors of strong-motion peaks obtained by the statistical analysis showed quite site-dependent variation, that is, they vary remarkably from site to site reflecting the difference in soil profile at each site. This indicates the importance of considering soil conditions peculiar to a site instead of the rough classification of soil types which have been employed by many researchers in the past.

An attenuation law for the peak acceleration, peak velocity and peak displacement on a rock was also obtained in terms of earthquake magnitude

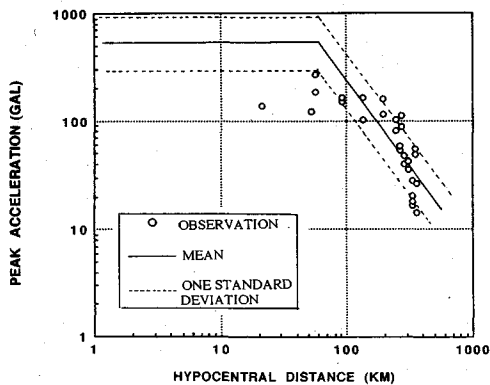


Fig.10 Comparison of peak acceleration at rock sites for the 1985 Michoacan earthquake with value predicted by the proposed semi-empirical model for $M=8.1$

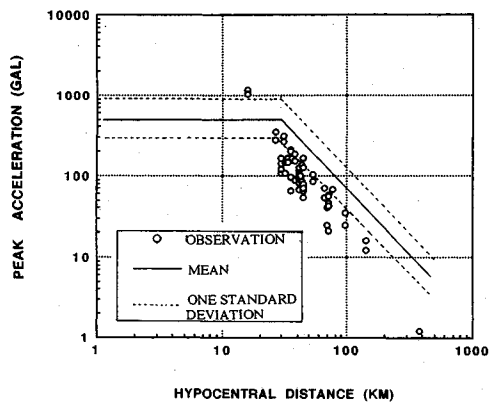


Fig.13 Comparison of peak acceleration at rock sites for the 1971 San Fernando earthquake with value predicted by the proposed semi-empirical model for $M=6.6$

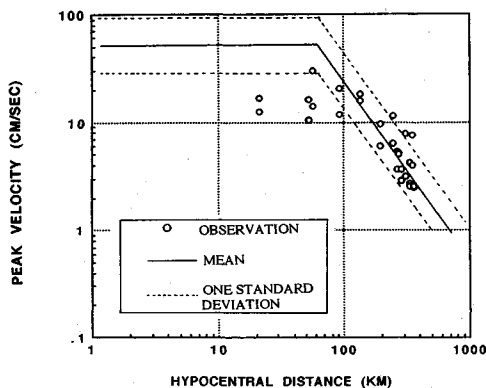


Fig.11 Comparison of peak velocity at rock sites for the 1985 Michoacan earthquake with value predicted by the proposed semi-empirical model for $M=8.1$

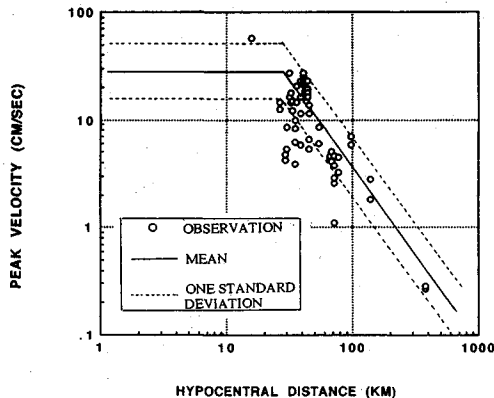


Fig.14 Comparison of peak velocity at rock sites for the 1971 San Fernando earthquake with value predicted by the proposed semi-empirical model for $M=6.6$

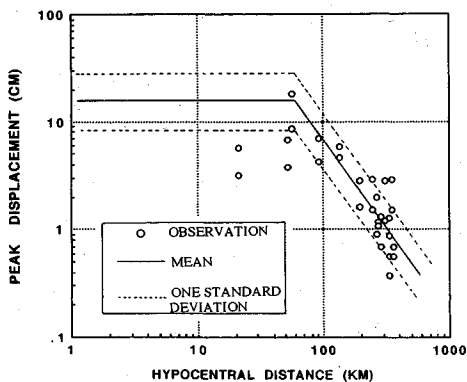


Fig.12 Comparison of peak displacement at rock sites for the 1985 Michoacan earthquake with value predicted by the proposed semi-empirical model for $M=8.1$

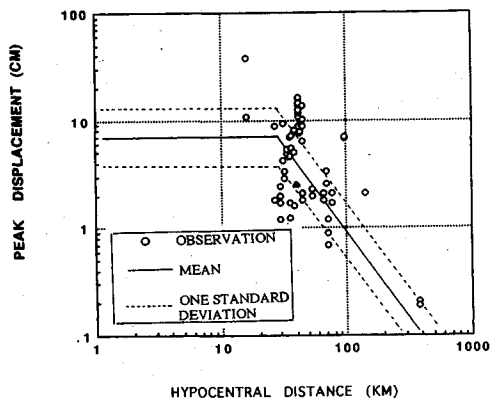


Fig.15 Comparison of peak displacement at rock sites for the 1971 San Fernando earthquake with value predicted by the proposed semi-empirical model for $M=6.6$

and hypocentral distance. The resulting attenuation law for peak values on a rock was successfully compared with strong-motion data observed during the 1989 Loma Prieta earthquake, the 1985 Michoacan earthquake and the 1971 San Fernando earthquake. Namely, it was shown that the proposed model predicts relatively well the observed data. In particular, we found a good agreement between the predicted and observed values in the comparisons of peak velocity. Since the proposed model was based solely on Japanese strong-motion data, this suggests that strong-motion peaks have a common attenuation law irrespective of country of origin on the assumption that there is little difference in each country's magnitude scale of earthquake.

ACKNOWLEDGMENTS

We thank the Port and Harbor Research Institute of the Ministry of Transport of Japan and the Public Works Research Institute of the Ministry of Construction of Japan for providing the strong-motion earthquake records used in this study. A part of this study was performed while the first author was a visiting professor at the Department of Civil and Environment Engineering, Rensselaer Polytechnic Institute. He has benefited greatly from collaboration and discussion with his colleagues. Special gratitude is extended to Prof. Papageorgiou who offered numerous suggestions for this study.

REFERENCES

- 1) Joyner, W.B. and Boore, D.M. : Measurement, Characterization and Prediction of Strong Ground Motion in Earthquake Engineering and Soil Dynamics, Vol.2 (Ed. J.L. Von Thun), ASCE, pp.103~155, 1988.
- 2) Campbell, K.W. : Strong Motion Attenuation Relations : Ten-Year Perspective, Earthquake Spectra, Vol.1, No.4, pp.759~804, 1985.
- 3) Kamiyama, M., M.J. O'Rourke and R. Flores-Berrones : A Semi-Empirical Analysis of Strong-Motion Peaks in Terms of Seismic Source, Propagation Path and Local Site Conditions, NCEER, Technical Report 92-0023.
- 4) Kanbayashi, Y. and Ichikawa, M. : A Method for

- Determining Magnitude of Shallow Earthquakes Occurring in and around Japan, Quarter Journal Seismology, Vol.41, pp.57~61, 1977 (in Japanese).
- 5) Aki, K. : Asperities, Barriers, Characteristic Earthquakes and Strong Motion Prediction, Journal Geophys. Res., Vol.89, No.B7, pp.5867~5872, 1984.
 - 6) Papageorgiou A.S. and Aki, K. : A Specific Barrier Model for the Quantitative Description of Inhomogeneous Faulting and the Prediction of Strong Ground Motion, Part 1 and Part 2, Bull. Seism. Soc. Am., Vol.73, pp.693~722, pp.953~978, 1983.
 - 7) Ida, Y. The Maximum Acceleration of Seismic Ground Motion, Bull. Seism. Soc. Am., Vol.63, pp.959~968, 1973.
 - 8) Chin B.H. and Aki, K. : Simultaneous Study of the source, Path, and Site Effects on Strong Ground Motion During the 1989 Loma Prieta Earthquake : A Preliminary Result on Pervasive Nonlinear Site Effects, Bull. Seism. Soc. Am., Vol.81, No.5, pp.1859~1884, 1991.
 - 9) Kamiyama, M. and Matsukawa, T. : An Empirical Scaling of Strong-Motion Spectra with Application to Estimate of Source Spectra, Structural Eng. and Earthq. Eng. (Proc. of Japan Soc. Civil Eng.), Vol.7, No.2, pp.331~342, 1990.
 - 10) Kamiyama, M. and Yanagisawa, E. : A Statistical Model for Estimating Response Spectra of Strong Earthquake Ground Motions With Emphasis on Local Soil Conditions, Soils and Foundations, Vol.26, No.2, pp.16~32, 1986.
 - 11) Tsuchida, H. et al. : Annual Report on Strong-Motion Earthquake Records in Japan Ports 1968~199, Technical Notes of the Port and Harbor Research Institute, No.98~No.649, The Port and Harbor Research Institute, Ministry of Transport, 1969~1990.
 - 12) Iwasaki, T. et al. : Strong-Motion Acceleration Records from Public Works in Japan No.1~No.8, Technical Notes of the Public Works Research Institute, Vol.32~38, The public Works Research Institute, Ministry of Construction, 1978~1983.
 - 13) Iai, S., Kurata, E. and Tsuchida, H. : Digitization and Correction of Strong-Motion Accelerograms, Technical Note of the Port and Harbor Research Institute, No.286 pp.5~56, 1978 (in Japanese).
 - 14) Sato, R., Theoretical Basis on Relationship Between Focal Parameters and Earthquake Magnitude, Journal Phys. Earth, Vol.27, pp.353~372, 1979.

(Received March 11, 1993)

強震地動の半経験的解析モデルとその予測手法の適用

神山 眞・マイケル オルーク・ラオル フローレスベロネス

強震地動の統計解析はそのデータセットの質と量において未だ限界がある。本論文ではこの限界を解決する一手法として理論的震源モデルを利用した半経験的解析モデルが導かれている。その誘導にあたっては、工学的応用の利便を考え、地震マグニチュードと震源距離という簡易パラメータが説明変数として用いられるとともに、観測点固有のローカルサイト効果が考慮されている。このモデルは日本で得られた強震記録 357 成分に適用され、最大地動の予測式が求められた。本モデルによる予測結果を 1989 年ロマプリータ地震を始め 3 個の代表的な外国の地震での観測結果と比較したところ比較的よい対応をみた。